SMASH, SENSE, PILS, GRAPPA

How to Choose the Optimal Method

Martin Blaimer, Felix Breuer, Matthias Mueller, Robin M. Heidemann, Mark A. Griswold, and Peter M. Jakob

Abstract: Fast imaging methods and the availability of required hardware for magnetic resonance tomography (MRT) have significantly reduced acquisition times from about an hour down to several minutes or seconds. With this development over the last 20 years, magnetic resonance imaging (MRI) has become one of the most important instruments in clinical diagnosis. In recent years, the greatest progress in further increasing imaging speed has been the development of parallel MRI (pMRI). Within the last 3 years, parallel imaging methods have become commercially available, and therefore are now available for a broad clinical use. The basic feature of pMRI is a scan time reduction, applicable to nearly any available MRI method, while maintaining the contrast behavior without requiring higher gradient system performance. Because of its faster image acquisition, pMRI can in some cases even significantly improve image quality. In the last 10 years of pMRI development, several different pMRI reconstruction methods have been set up which partially differ in their philosophy, in the mode of reconstruction as well in their advantages and drawbacks with regard to a successful image reconstruction. In this review, a brief overview is given on the advantages and disadvantages of present pMRI methods in clinical applications, and examples from different daily clinical applications are shown.

Key Words: MRI, parallel imaging, SMASH, SENSE, PILS, GRAPPA

Besides the image contrast, imaging speed is probably the most important consideration in clinical magnetic resonance imaging (MRI). Unfortunately, current MRI scanners already operate at the limits of potential imaging speed because of the technical and physiologic problems associated with rapidly switched magnetic field gradients. With the appearance of parallel MRI (pMRI), a decrease in acquisition time can be achieved without the need of further increased gradient performance.

pMRI works by taking advantage of spatial sensitivity information inherent in an array of multiple receiver surface-coils to partially replace time-consuming spatial encoding, which is normally performed by switching magnetic field gradients. In this way, only a fraction of phase-encoding steps have to be acquired, directly resulting in an accelerated image acquisition while maintaining full spatial resolution and image contrast. Besides increased temporal resolution at a given spatial resolution, the time savings due to pMRI can also be used to improve the spatial resolution in a given imaging time. Furthermore, pMRI can diminish susceptibility-caused artifacts by reducing the echo train length of single- and multi-shot pulse sequences.

Currently, the newest generation of MRT scanners provide up to 32 independent receiver channels, which theoretically allow a 32× increased image acquisition speed compared with traditional MR systems without pMRI environment. At the moment, however, clinical routine experiments can only be accelerated by a factor 2 to 4, resulting in very good image quality. Higher scan time reductions can be achieved in three-dimensional (3D) experiments (acceleration factors 5–8) where the number of phase-encoding steps can be reduced in two spatial dimensions. Further scan time reductions have been obtained at research sites using specialized hardware (acceleration factors 9–12). These new generation MRI scanners with pMRI have provided the greatest incremental gain in imaging speed since the development of fast MRI methods in the 1980s.

Over the last 10 years, great progress in the development of pMRI methods has taken place, thereby producing a multitude of different and somewhat related parallel imaging reconstruction techniques and strategies.[1–10] Currently, the most well known are SMASH,[1] SENSE,[2] and GRAPPA.[3] However, various other techniques, such as AUTO-SMASH,[4] VD-AUTO-SMASH,[5] GENERALIZED SMASH,[6] MSENSE,[7] PILS,[8] and SPACE RIP[9] have also been proposed. All these techniques require additional coil sensitivity information to eliminate the effect of undersampling the k-space. This sensi-

tivity information can be derived either once during the patient setup by means of a prescan or by means of a few additionally acquired k-space lines for every subsequent pMRI experiment (autocalibration), or some combination of the two. The present pMRI reconstruction methods can roughly be classified into two groups. Those in which the reconstruction takes place in image space (eg, SENSE, PILS) consist of an unfolding or inverse procedure and those in which the reconstruction procedure is done in k-space (eg, SMASH, GRAPPA), consist of a calculation of missing k-space data. However, hybrid techniques like SPACE RIP are also conceivable.

There are many applications that have already seen remarkable benefits from the enhanced image acquisition capabilities of pMRI, such as head, thoracic, and cardiac imaging. But which pMRI method is best suited for any given clinical application?

This review article is an attempt to give some answers to this question and might help a clinician to choose the optimal pMRI method for a specific application. At the beginning, a brief technical overview of the existing pMRI methods is given. Differences, similarities, advantages, and disadvantages will be discussed. However, the main focus will be put on the two present commercially available techniques, SENSE and GRAPPA.

Technical Overview of Current pMRI Methods

In this article, a brief technical overview over the present pMRI reconstruction methods and strategies is given. However, to keep things as simple as possible, we confine ourselves to Cartesian-type sampled k-space, in which the number of phase-encoding steps is reduced by the reduction factor R by increasing the distance of equidistantly sampled k-space lines. To maintain resolution, the maximal k-values are left unchanged. In image space, this type of undersampling the k-space yields in a reduced field of view (FOV) in phase-encoding direction associated with foldover artifacts in the coil images as depicted in Figure 1.

To provide a simple idea how pMRI operates, a simplified idealized example is given. Afterwards, the PILS method is introduced, which extends the simplified example into a real-world situation. Following this, the basics of SENSE will be presented. It is shown that SENSE can be seen as an "unfolding" algorithm in image domain. Thereafter, the development of k-space-related pMRI methods is described. Starting with basic SMASH theory, the development of autocalibrated pMRI techniques, such as AUTO-SMASH, VD-AUTO-SMASH, and GRAPPA, is presented. Finally, SPACE RIP as a hybrid technique is mentioned.

pMRI: A Simplified Example

To provide an intuitive comprehension of how an array of multiple receiver coils can be used to accelerate image acquisition, we begin with a simplified example.
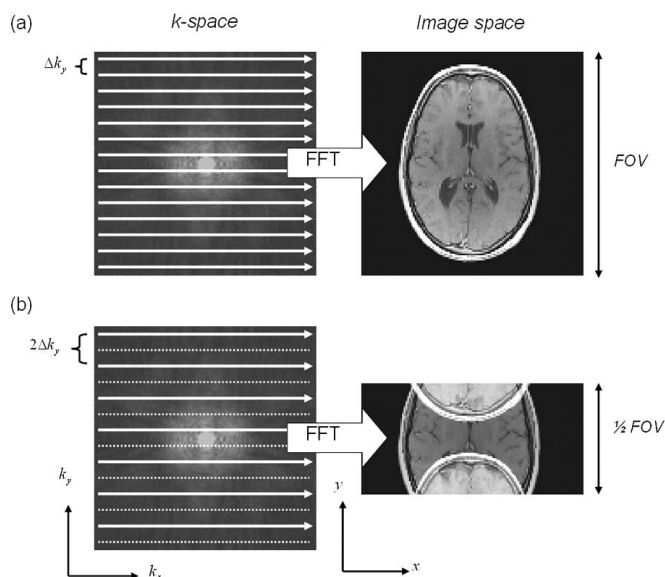

FIGURE 1. A, Conventional acquisition of fully sampled k-space, resulting in a full FOV image after Fourier transformation. B, Undersampled acquisition ($R = 2$), resulting in a reduced FOV (FOV/2) with aliasing artifacts. Solid lines indicate acquired k-space lines, dashed lines indicate nonacquired k-space lines.

Let us assume we have an array of $N_c = 2$ independent receiver coils, each covering one half of the FOV with a box-car-type sensitivity profile C_k in phase-encoding direction (Fig. 2b). In this idealized setup, coil 1 detects only the top half of the object (Fig. 2c), whereas coil 2 detects only the bottom half of the object (Fig. 2d). A normal acquisition with just a single homogeneous volume coil would require N phase-encoding steps for a full FOV image of the object (Fig. 2a). Using the identical imaging parameters in the depicted two-coil situation, the resulting component coil images provide full FOV images with signal originating only according to the individual boxcar sensitivity profiles. In other words, coil 1 covers only one (half) part of the object in the full FOV image, while receiving no signal from the other (half) part of the object, while the opposite applies to coil 2.

This fact can be used to halve the FOV, which means reducing the number of phase-encoding steps by a factor of $R = 2$. As a result, two half FOV component coil images are simultaneously obtained in half the imaging time (Fig. 2e). Thus, the distinctiveness of the involved coil sensitivities allows a parallel imaging process.

In a final reconstruction step, the component coil images can easily be combined to one full FOV image with full resolution by appropriately shifting the individual coil images (Fig. 2f). This final image is then obtained in half of the imaging time (reduction factor $R = 2$). The resulting signal-to-noise ratio (SNR) in the accelerated pMRI acquisition is reduced by a
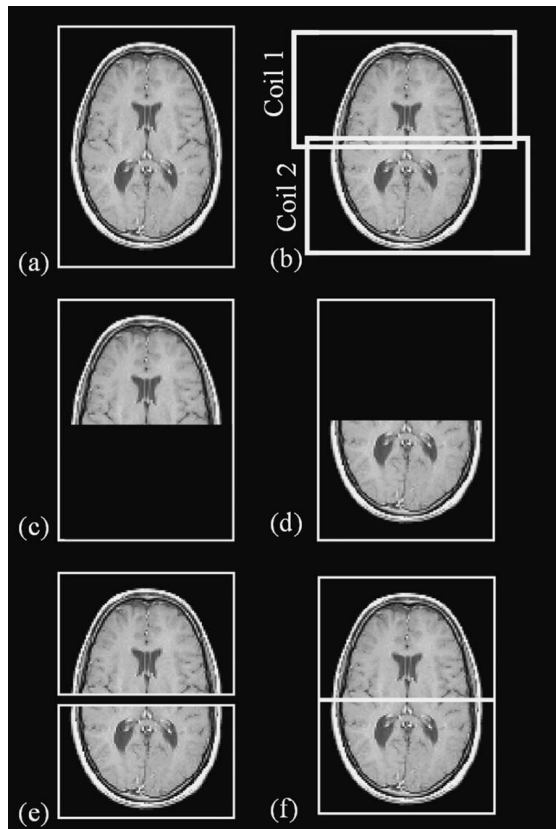
FIGURE 2. A, Full FOV image with *N* phase-encoding steps (one homogeneous coil). B, Two-coil array with boxcar-type sensitivity profile. C, Full FOV image with *N* phase-encoding steps received in coil 1. D, Full FOV image with *N* phase-encoding steps received in coil 2. E, FOV/2 image with *N/2* phase-encoding steps received in coil 1 (*top*) and in coil 2 (*bottom*). F, Combined coil images with full FOV and *N/2* phase-encoding steps.

tion. In this case, each receiver coil has a completely localized sensitivity with each coil having sensitivity over a distinct region Y_c and zero elsewhere (Fig. 3a). According to the localized sensitivities, each coil covers a distinct region of the object in the full FOV image (Fig. 3b). An accelerated pMRI acquisition with a reduced FOV in phase-encoding direction will result in periodically repeating subimages (Fig. 3c). However, as long as the reduced FOV Y_i is chosen to be larger than the finite sensitivity region ($Y_c < Y_i < Y$), the subimages appear totally separated in the full FOV, whereas the position of the correct subimage is lost. By means of the knowledge of the exact position of the individual coils in the linear array, we are able to extract the corresponding subimage at the correct position for each coil (Fig. 3d). Finally, these subimages (Fig. 3e) can be combined to build a full FOV image with full resolution (Fig. 4f). PILS is restricted to an adequate coil arrangement, where the individual coils are placed over the FOV in phase-encoding direction. PILS achieves optimal SNR, which means that SNR is only reduced by the expected factor $\sqrt{R}$. Further
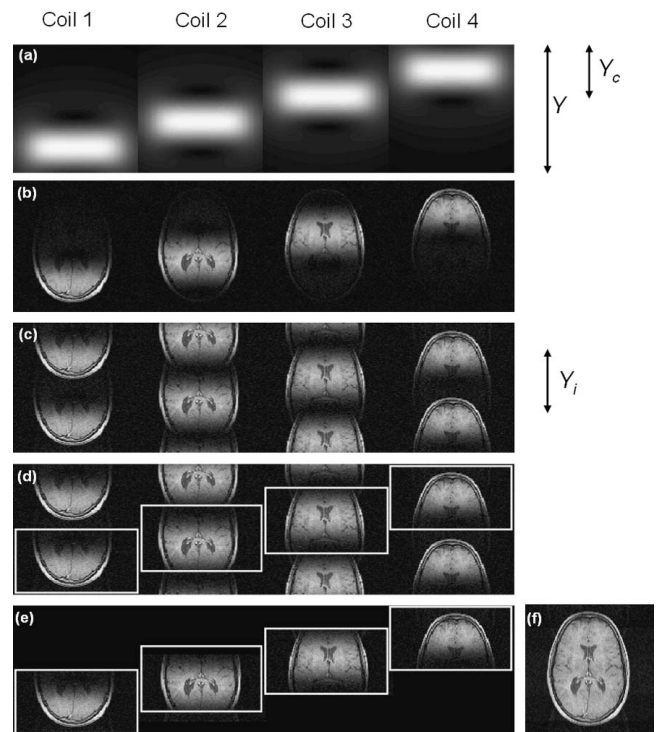

FIGURE 3. A, Receiver coils positioned linear in phase-encoding direction with localized sensitivities over distinct regions Y_c in the full FOV image *Y*. B, Corresponding full FOV coil images and the (C) reduced FOV Y_i coil images. As long as $Y_c < Y_i < Y$, the subimages appear totally separated in the full FOV *Y*, whereas the position of the correct subimages is lost. D, By means of the exact knowledge of the coil position in the full FOV, the correct subimages of each coil can be extracted (E) and finally combined to build (F) a full FOV image of the object with full resolution.

factor $\sqrt{R}$, since the number of acquired phase-encoding steps is reduced by a factor *R*.

This simplified and idealized example does not reflect a real-world situation, where coil sensitivities *C* are smooth over the FOV and normally overlap to some extent. However, this simple example provides an intuitive grasp of pMRI and outlines most of its important requirements and properties.

(1) Multiple receiver coils with different coil sensitivities over the FOV are required.
(2) Each coil must be provided with its own receiver pathway.
(3) For pMRI reconstruction, an accurate knowledge of the coil sensitivities is required.

The SNR of the accelerated pMRI image is at least reduced by a factor $\sqrt{R}$.

Partially Parallel Imaging With Localized Sensitivities (PILS)

The PILS reconstruction method extends the prior considerations of the idealized world above to a real-world situa-
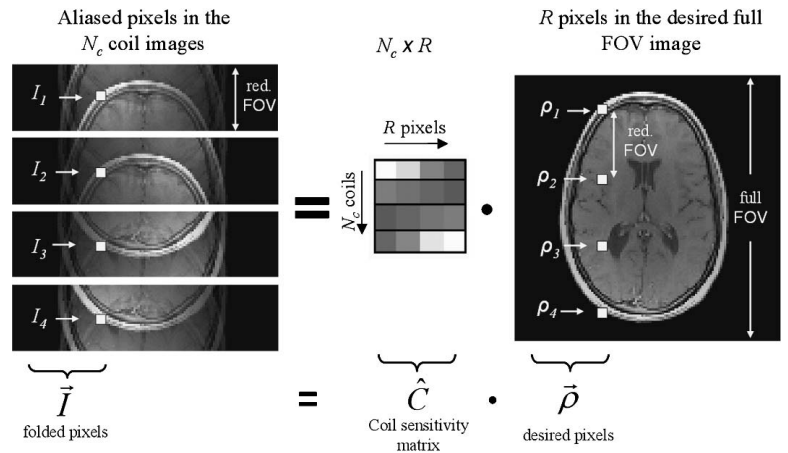
FIGURE 4. Illustration of the basic SENSE relation using an accelerated ($R = 4$) pMRI acquisition with $N_c = 4$ receiver coils. $\vec{I}$ contains the aliased pixels at a certain position in the reduced FOV coil images. The sensitivity matrix $\hat{C}$ assembles the corresponding sensitivity values of the component coils at the locations of the involved ($R = 4$) pixels in the full FOV image $\vec{\rho}$.

losses in SNR do not arise because the final image is composed of shifted versions of reduced FOV images. It should be clear that PILS is strongly restricted to coil configurations with localized sensitivities. In the next sections, more generalized methods will be discussed.

Sensitivity Encoding (SENSE)

The SENSE pMRI reconstruction method can briefly be characterized as an image domain "unfolding" algorithm. In the Cartesian-type sampled k-space, the location of and distance between periodic repetitions in image domain are well known. A pMRI accelerated acquisition (reduction factor R) results in a reduced FOV in every component coil image. Each pixel in the individual reduced FOV coil image will contain information from multiple (R), equidistantly distributed pixels in the desired full FOV image. Additionally, these pixels will be weighted with the coil sensitivity C at the corresponding location in the full FOV. Thus, the signal in one pixel at a certain location *(x,y)* received in the *k*'th component coil image I_k can be written as

$$I_k(x, y) = C_k(x, y_1)\rho(x, y_1) + C_k(x, y_2)\rho(x, y_2)$$
$$+ \cdots + C_k(x, y_R)\rho(x, y_R). \qquad (1)$$

With index k counting from 1 to N_c and index l counting from 1 to R, specifying the locations of the pixels involved, Equation 1 can be rewritten to

$$I_k = \sum_{l=1}^{N_p} C_{kl}\rho_l. \qquad (2)$$

Including all N_c coils, a set of (N_c) linear equations with (R) unknowns can be established and transformed in matrix notation:

$$\vec{I} = \hat{C} \cdot \vec{\rho} \qquad (3)$$

As shown in Figure 4, the vector $\vec{I}$ represents the complex coil image values at the chosen pixel and has length N_c. The matrix $\hat{C}$ denotes the sensitivities for each coil at the R superimposed positions and therefore has the dimension $N_c \times R$. The vector $\vec{\rho}$ lists the R pixels in the full FOV image. Using proper knowledge of the complex sensitivities at the corresponding positions, this can be accomplished using a generalized inverse of the sensitivity matrix $\hat{C}$.

$$\vec{\rho} = (\hat{C}^H \hat{C})^{-1} \hat{C}^H \cdot \vec{I} \qquad (4)$$

To simplify matters, the issue of noise correlation is not addressed in Equation 4. However, to account for levels and correlations of stochastic noise in the received data, terms may be included to deal with this correlation. This can be especially important when the receiver coils are not completely decoupled. A detailed description is given by Pruessmann et al.[2]

The "unfolding" process in Equation 4 is possible as long as the matrix inversion in Equation 4 can be performed. Therefore, the number of pixels to be separated R must not exceed the number of coils N_c in the receiver array. The SENSE algorithm (Equation 4) has to be repeated for every pixel location in the reduced FOV image to finally reconstruct the full FOV image. In contrast to PILS, SENSE provides pMRI with arbitrary coil configurations, however, at the expense of some additional SNR loss, which depends on the underlying geometry of the coil array. The encoding efficiency at any position in the FOV with a given coil configuration can be analytically described by the so-called geometry factor (g-factor), which is a measure of how easily the matrix inversion in Equation 4 can be performed. Thus, the SNR in the final SENSE image is additionally reduced by the g-factor compared with PILS.

$$SNR_{SENSE} = \frac{SNR_{full}}{\sqrt{R} \cdot g} \qquad (5)$$

FROM SMASH TO GRAPPA

SMASH

Like SENSE, pure SMASH (Simultaneous Acquisition of Spatial Harmonics) at its basic level requires a prior estimation of the individual coil sensitivities of the receiver array. The basic concept of SMASH is that a linear combination of these estimated coil sensitivities can directly generate missing phase-encoding steps, which would normally be performed by using phase-encoding magnetic field gradients. In this case, the sensitivity values $C_k(x,y)$ are combined with appropriate linear weights $n_k^{(m)}$ to generate composite sensitivity profiles C_m^{comp} with sinusoidal spatial sensitivity variations of the order m (Fig. 5):

$$C_m^{comp}(x, y) = \sum_{k=1}^{N_c} n_k^{(m)} C_k(x, y) \cong e^{im\Delta k_y y} \qquad (6)$$

Here, $\Delta k_y = 2\pi/FOV$ and index k counts from 1 to N_c for an N_c-element array coil, while m is an integer, specifying the order of the generated spatial harmonic. With this, the only unknowns in the linear equation are the linear weights $n_k^{(m)}$, which can be estimated by fitting (eg, least square fit) the coil sensitivity profiles C_k to the spatial harmonic $e^{im\Delta k_y y}$ of order m. The component coil signal $S_k(k_y)$ in one dimension (phase-encoding direction), which is received in coil k, is the Fourier transformation of the spin density $\rho(y)$ weighted with the corresponding coil sensitivity profile $C_k(y)$:

$$S_k(k_y) = \int dy \rho(y) C_k(y) e^{ik_y y} \qquad (7)$$

Using Equations 6 and 7, we may derive an expression to generate shifted k-space lines $S(k_y + m\Delta k_y)$ from weighted combinations of measured component coil signals $S_k(k_y)$.

$$\sum_{k=1}^{N_c} n_k^{(m)} \cdot S_k(k_y) = \int dy \rho(y) \sum_{k=1}^{N_c} n_k^{(m)} C_k(y) e^{ik_y y}$$

$$\cong \int dy \rho(y) e^{im\Delta k_y y} e^{ik_y} = S^{comp}(k_y + m\Delta k_y)$$

$$(8)$$

Equation 8 represents the basic SMASH relation and indicates that linear combinations of component coils can actually be used to generate k-space shifts in almost the same manner as magnetic field gradients in conventional phase-encoding. In general, though, SMASH is strongly restricted to coil configurations that are able to generate the desired spatial harmonics in phase-encoding direction with adequate accuracy.
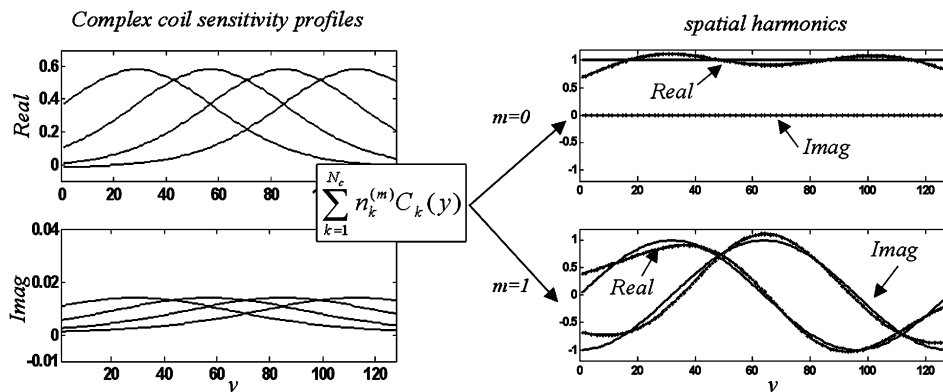
Auto-SMASH and VD-AUTO-SMASH

In contrast to a prior estimation of component coil sensitivities, AUTO-SMASH uses a small number of additionally acquired autocalibration signal (ACS) lines during the actual scan to estimate the sensitivities. An AUTO-SMASH type acquisition scheme is shown in Figure 6c for a reduction factor $R = 3$. In general, $R - 1$ extra ACS lines are required, which are normally placed in the center of k-space at positions $m\Delta k_y$, where m counts from 1 to $R - 1$. In contrast to normal SMASH, these additionally acquired ACS lines S_k^{ACS} are used to automatically derive the set of linear weights $n_k^{(m)}$.

In the absence of noise, the combination of the weighted profiles at (k_y) of the component coil images that represents a k-space shift of $m\Delta k_y$ must yield the weighted (by the 0th harmonic factor) combined autocalibration profile obtained at $k_y + m\Delta k_y$.

$$S^{comp}(k_y + m\Delta k_y) = \sum_{k=1}^{N_c} S_k^{ACS}(k_y + m\Delta k_y) \cong \sum_{k=1}^{N_c} n_k^{(m)} S_k(k_y)$$

$$(9)$$

By fitting the component coil signals $S_k(k_y)$ to the composite signal $S^{comp}(k_y + m\Delta k_y)$, which are composed of ACSs $S_k^{ACS}(k_y + m\Delta k_y)$, a set of linear weights $n_k^{(m)}$ may again be derived, which can shift measured lines by $m\Delta k_y$ in k-space. In this way, missing k-space data can be calculated from measured k-space data to form a complete dense k-space, resulting in a full FOV image after Fourier transformation.

FIGURE 5. Illustration of the basic SMASH relation. The complex sensitivity profiles $C_k(y)$ from a 4-element ideal array (*left*) are fit to spatial harmonics (*solid lines*) of order $m = 0$ (*right top*) and $m = 1$ (*right bottom*). The dotted lines represent the best possible approximation of the spatial harmonics with the underlying coil array.
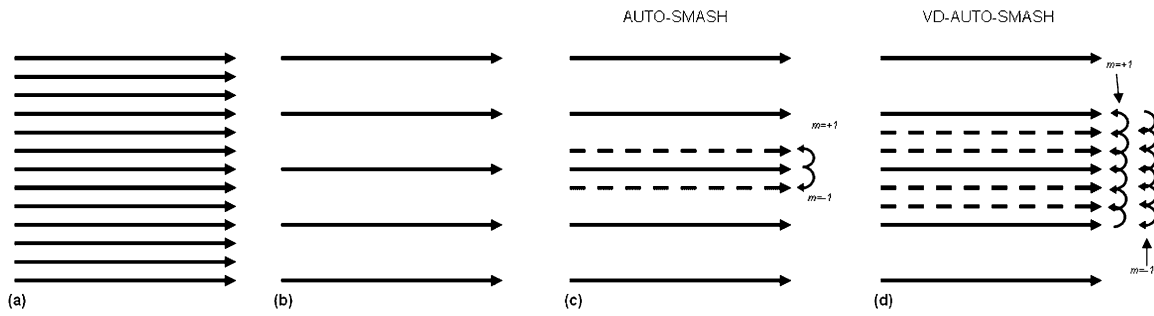
FIGURE 6. (A) Fully Fourier encoded k-space (R = 1), (B) undersampled (R = 3) k-space without ACS lines, (C) AUTO-SMASH-type undersampled (R = 3) k-space with two additional ACS lines to derive the coil weights for a k-space shift of $+\Delta k$ (m = +1) and $-\Delta k$ (m = −1) and (D) VD-AUTO-SMASH-type undersampled (R = 3) k-space with multiple additional ACS lines to derive the coil weights for a k-space shift of $+\Delta k$ (m = +1) and $-\Delta k$ (m = −1) more accurately.

The concept of variable-density (VD)-AUTO-SMASH was introduced as a way to further improve the reconstruction procedure of the AUTO-SMASH approach. In this method, multiple ACS lines are acquired in the center of k-space. Figure 6d schematically depicts a VD-AUTO-SMASH type acquisition with a threefold undersampled (outer) k-space. This simple examples demonstrates that the number of available fits with which one can derive the weights for the desired k-space shifts (m = +1, −1) is significantly increased just by adding a few extra ACS lines to the acquisition. Furthermore, these reference data can be integrated in a final reconstruction step to further improve image quality. It has been shown[5] that the VD-AUTO-SMASH approach provides the best suppression of residual artifact power at a given total acceleration factor R, using the maximum possible undersampling in the outer k-space in combination with the highest possible number of ACS lines in the center of k-space. This strategy results in a more accurate determination of the reconstruction coefficients, especially in the presence of noise and a more robust image reconstruction in the presence of imperfect coil performance.

GeneRalized Autocalibrating Partially Parallel Acquisitions (GRAPPA)

GRAPPA represents a more generalized implementation of the VD-AUTO-SMASH approach. Although both techniques share the same acquisition scheme, they differ significantly in the way reconstruction of missing k-space lines is performed. One basic difference is that the component coil signals $S_k(k_y)$ are fit to just a single component coil ACS signal $S_l^{ACS}(k_y + m\Delta k_y)$, not a composite signal, thereby deriving the linear weights to reconstruct missing k-space lines of each component coil:

$$S_l^{ACS}(k_y + m\Delta k_y) \cong \sum_{k=1}^{N_c} n_k^{(m)} S_k(k_y) \qquad (10)$$

This procedure needs to be repeated for every component coil, and since the coil sensitivities change also along read direction, the weights for the GRAPPA reconstruction are normally determined at multiple positions along read direction. After Fourier transformation, uncombined images for each single coil in the receiver array are obtained. Furthermore, unlike VD-AUTO-SMASH, GRAPPA uses multiple k-space lines from all coils to fit one single coil ACS line, resulting in a further increased accuracy of the fit procedure (ie, over determined system) and therefore in better artifact suppression. A schematic description of an R = 2 VD-AUTO-SMASH and GRAPPA reconstruction procedure is given in Figure 7.

The GRAPPA reconstruction formalism can also be written in matrix form. The vector $\vec{S}$ represents the collected signal in each element coil at some position k and therefore has length N_c. Using GRAPPA in its simplest form, a set of weights $\hat{n}^{(m)}$ can be derived by fitting the signal $\vec{S}$ to the ACS at the position $k + m\Delta k$ in each coil. Therefore, the coil-weighting matrix $\hat{n}^{(m)}$ has the dimension $N_c \times N_c$ and may shift the k-space data in each coil by $m\Delta k$.

$$\vec{S}^{(m)} = \hat{n}^{(m)} \vec{S} \qquad (11)$$

In contrast to a SMASH or VD-AUTO-SMASH complex sum image reconstruction, the GRAPPA algorithm results in uncombined single coil images, which can be combined using a magnitude reconstruction procedure (eg, sum of squares). This provides a significantly improved SNR performance, especially at low reduction factors. Furthermore, signal losses due to phase cancellations are essentially eliminated using a magnitude reconstruction procedure. Thus, previous drawbacks on k-space-based techniques, namely, phase cancellation problems, low SNR, and poor reconstruction quality due to a suboptimal fit procedure, are essentially eliminated. Furthermore, similar to SENSE, the GRAPPA algorithm works with essentially arbitrary coil configurations. Finally, as

FIGURE 7. Schematic description of an accelerated (R = 2). A, AUTO-SMASH and VD-AUTO-SMASH reconstruction process. Each dot represents a line in k-space in a single coil of the receiver array. A single line from all coils is fit to a single ACS line in a sum-like composite k-space. B, GRAPPA uses multiple lines from all coils to fit one line in one coil (here coil 4). This procedure needs to be repeated for every coil, resulting in uncombined coil images, which can be finally combined using a sum of squares reconstruction.
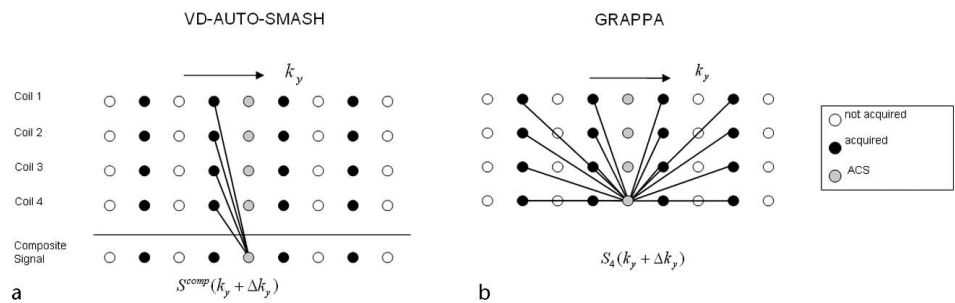
an additional benefit, ACS lines used to derive the reconstruction coefficients can in many cases be integrated into the final image reconstruction, in the same manner as intended in VD-AUTO-SMASH. The image series in Figure 8 depicts the temporal evolution of k-space-related pMRI reconstruction algorithms in terms of image quality for one particular example. It is shown that pure SMASH (Fig. 8b) suffers from signal losses due to phase cancellations and often results in residual artifacts when the underlying coil array is not able to generate accurate spatial harmonics. With the advent of AUTO-SMASH (Fig. 8c), a self-calibrated pMRI reconstruction method was introduced, which is still affected by the limitations of SMASH imaging. With the development of VD-AUTO-SMASH (Fig. 8d), a more accurate estimation of the coil weights was achieved, resulting in a better suppression of residual artifacts. Finally, with GRAPPA (Fig. 8e), the accuracy of the coil weights was further improved. The GRAPPA-type coil-by-coil reconstruction process additionally eliminates the drawbacks of signal cancellations and low SNR, since the resulting

uncombined coil images can be combined using a normal sum of squares reconstruction.

Sensitivity Profiles From an Array of Coils for Encoding and Reconstruction In Parallel (SPACE RIP)

The SPACE RIP technique also (like SENSE and SMASH) requires an initial estimation of the two-dimensional sensitivity profiles of each component coil in the receiver array. In principle, SPACE RIP uses the same basic building blocks of the SENSE reconstruction but works in k-space to do the image reconstruction. This allows one to use a variable density sampling scheme similar to VD-AUTO-SMASH and GRAPPA in a very easy way. It has been shown[9] that this variable density sampling scheme can improve the SNR of the reconstructed image significantly. In combination with a non-Cartesian sampling grid or with the variable density approach, SPACE RIP produces big matrices that need to be inverted, and this can be very time consuming.
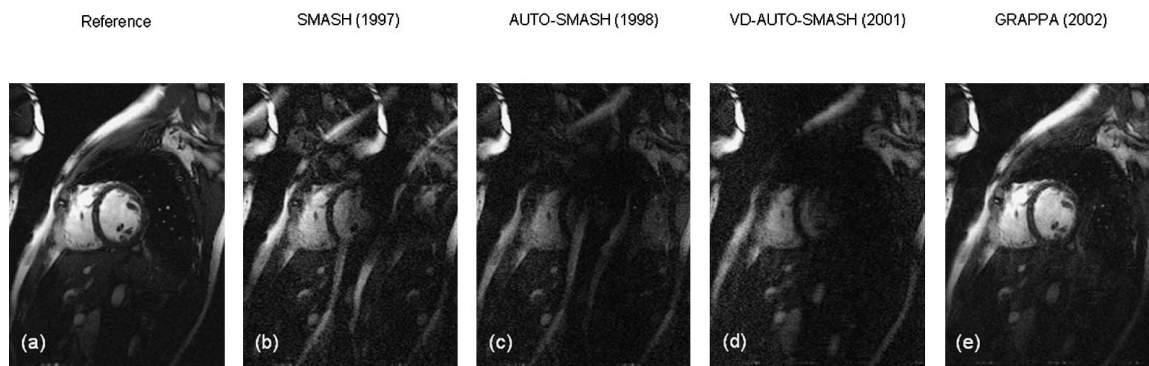

FIGURE 8. Comparison of R = 2 accelerated acquisitions of the human heart using (B) pure SMASH, (C) AUTO-SMASH, (D) VD-AUTO-SMASH, and (E) GRAPPA for image reconstruction. The image series represents the evolution of the k-space related pMRI reconstruction algorithms. It is shown that a continuous improvement of image quality has been achieved over the years. It can be seen that GRAPPA results in a very good image quality without phase cancellation problems, without residual artifacts, and with optimized SNR, since GRAPPA allows a sum of squares reconstruction of the uncombined component coil images. As a comparison (A), a full FOV acquisition is shown.

Sensitivity Assessment

As mentioned before, a successful SENSE, SMASH, and SPACE RIP reconstruction is strongly associated with an accurate knowledge of the coil sensitivities. Since the sensitivity varies with coil loading, the sensitivities must be accessed by an additional reference acquisition integrated in the actual imaging setup. This can be done, for example, by a low resolution fully Fourier-encoded 3D acquisition received in each component coil, which allows arbitrary slice positioning and slice angulations. Thus, sensitivity maps can be derived by either one of these methods

(1) dividing each component coil image by an additional body coil image.[2]
(2) dividing each component coil image by a "sum of square" image including phase modulation.[11]
(3) dividing each component coil image by one component coil image (relative sensitivity maps).[12]
(4) an adaptive sensitivity assessment based on the correlation between the component coil images.[13]

In an additional numerical process, these raw-sensitivity maps need to be refined using smoothing (ie, minimizing the propagation of additional noise from the calibration scan into the reconstructed image) and extrapolation algorithms (ie, to provide coils sensitivity information from regions where MR signal is hard to obtain).

Autocalibration

The concept of autocalibration was first presented by Jakob et al[4] in 1998 who introduced the AUTO-SMASH technique. The philosophy of autocalibration differs significantly from other approaches in which the sensitivity information is derived only once already during the patient setup (eg, prescan). Autocalibration may imply acquisition of reference signals directly in front of, during, or directly after the actual pMRI experiment. This is beneficial because the accurate knowledge of the spatial sensitivity information of the underlying coil array is a crucial element in pMRI and it is difficult to ensure that patient and coil position remain unchanged during the entire clinical protocol, especially when using flexible array coils or when patient motion is inevitable (eg, respiratory motion, uncooperative patients). In general, an inaccurate estimation of coil sensitivity information will result in bad image quality. Therefore, the autocalibration concept can in many cases provide a more robust pMRI reconstruction. In addition, the ACS lines can be integrated into the final image in most cases, thereby additionally improving image quality by reducing residual artifact power and increasing SNR.

Please note that the concept of autocalibration is not restricted to k-space-related pMRI reconstruction methods because, in principle, one can use the ACS lines required for a GRAPPA reconstruction as well to derive low-resolution coil sensitivity maps for SENSE reconstructions within every sub-

sequent pMRI experiment. This is done, for example, in the mSENSE[7] method.

Coil Arrangement Considerations

In principle, both commercially available techniques, SENSE and GRAPPA, allow an arbitrary coil configuration around the object. This means that these techniques are not restricted to linear coil configurations or localized sensitivities. However, coil sensitivity variation in the phase-encoding direction in which the reduction is performed must be ensured. The geometry factor (g-factor) analytically describes the local noise enhancement in the final SENSE image when using a given coil configuration. Therefore, the g-factor represents an easy way to estimate the encoding efficiency of a receiver array. In general, to optimize a coil configuration for a specific application, one should simulate g-factors for several coil configurations. Although, the g-factor actually represents a quantitative estimation of noise enhancement only for a SENSE reconstruction, we have found that g-factor estimation works for GRAPPA as well, since GRAPPA is subject to the same requirements in terms of coil configuration.

A Comparison: SENSE Versus GRAPPA

Because of their availability for daily clinical routine, the following section addresses advantages and disadvantages of both SENSE and GRAPPA. Although both methods are different approaches to reconstruct missing data, they provide very good results with nearly identical reconstruction quality, as illustrated in Figure 9, and are therefore well suited to enhance almost every clinical application.

To date, the most widespread used pMRI technique is SENSE, which is offered by many companies in slightly modi-
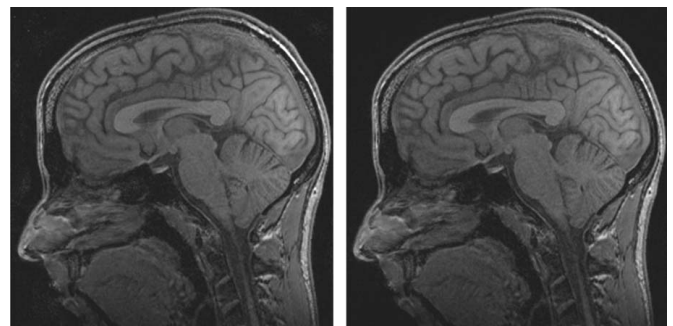
(a)   **(b)**

FIGURE 9. Comparison of the image quality of SENSE and GRAPPA reconstructions with a reduction factor of three. A, With accurate coil sensitivity maps, the SENSE reconstruction obtains the best possible result with optimized SNR. B, The GRAPPA reconstruction is an approximation to the SENSE reconstruction. Yet on the visual scale, no differences can be seen between both methods.

fied implementations: Philips (SENSE), Siemens (mSENSE), General Electric (ASSET), Toshiba (SPEEDER).

Because of the broad availability of SENSE, this technique has become the most used parallel imaging method in the clinical routine. Many clinical applications already benefit from the enhanced image acquisition capabilities of SENSE.

For example, in cardiac imaging, the scan time reduction due to SENSE relaxes the requirements for breath-hold studies. Optionally, the gain in scan time can be used to improve the spatial resolution.[14] Furthermore, because of the reduced imaging time, real-time cardiac imaging without ECG triggering or breath-holding can be realized.[15]

Another example for the application of SENSE is contrast-enhanced magnetic resonance angiography (CE-MRA). The most critical parameter for CE-MRA is the imaging time because the total acquisition has to be completed during the first pass of the contrast agent and therefore the spatial resolution of CE-MRA is restricted. SENSE enables a higher spatial resolution at constant scan time or a time-resolved CE-MRA study, consisting of multiple 3D data sets acquired during the passage of the contrast agent.[16]

A particular example of a clinical application that can benefit from the increased imaging speed provided by parallel imaging is head MRI. Single-shot and turbo spin-echo sequences, such as TSE and HASTE, are commonly used for *T2*-weighted brain imaging. The application of pMRI can be used to effectively reduce blurring due to the *T2* relaxation and therefore improves the image quality of these sequences.[17] Besides *T2*-weighted imaging with TSE sequences, single-shot echo-planar imaging (EPI) has become the clinical standard in areas such as functional MRI, diffusion-tensor imaging for fiber tracking, and diffusion-weighted MRI, which is an important diagnostic tool for the examination of patients with acute stroke. Combining single-shot EPI with SENSE has been shown to reduce the disadvantages of EPI, namely, the blurring and signal losses due to the *T2**-based signal decay during read-out and distortions in the reconstructed image caused by off-resonance spins.[18,19]

For breast imaging, magnetic resonance in combination with parallel imaging is a powerful diagnostic tool, which also yields functional information about a breast cancer's biologic behavior and might become a standard, frequently used, clinical study in the near future. In particular, dynamic contrast-enhanced breast MRI benefits from a higher spatial resolution at a given scan time provided by SENSE.[20] The increased spatial resolution allows the visualization of high anatomic detail and therefore delivers an increased diagnostic specificity.

The only regenerative k-space technique commercially available at the moment is GRAPPA. The reason for offering two different pMRI methods is that there are a number of clinical applications in which the use of GRAPPA is advantageous. Examples include lung and abdominal MRI,[21,22] real-time imaging,[23] and the application for single-shot techniques.[24]

Parallel imaging with GRAPPA is particularly beneficial in areas where accurate coil sensitivity maps may be difficult to obtain. In inhomogeneous regions with low spin density such as the lung and the abdomen, it can be difficult to determine precise spatial coil sensitivity information. In these regions, the image quality of SENSE reconstructions might therefore suffer from inaccurate sensitivity maps. In contrast, the GRAPPA algorithm provides good quality image reconstructions,[21,22] since the sensitivity information is extracted from the k-space. In GRAPPA, central k-space lines are fit to calculate the reconstruction parameters. This fitting procedure involves global information and is therefore not affected by localized inhomogeneities. The use of lines near the center of k-space also ensures that there is sufficient information to achieve a good reconstruction quality. In Figure 10, the use of the GRAPPA approach for lung imaging is illustrated.

Another application where accurate coil sensitivity maps may be difficult to derive is single-shot EPI. Single-shot EPI has become the clinical standard in areas such as functional MRI and diffusion-weighted MRI. Yet, in addition to *T2* or *T2**-related blurring and signal losses found in all single-shot imaging techniques, EPI has the additional problem of image distortions originating from susceptibility-related off-resonance spins. The fractional displacement $\Delta S/S$ due to distortions can be determined by the off-resonance frequency Δf and the interecho spacing T_{inter} and is given by:

$$\frac{\Delta S}{S} = \Delta f \cdot T_{\mathrm{inter}} \qquad (12)$$

The effective interecho spacing and therefore the distortions are reduced by the use of pMRI, without the need of several excitations as in segmented EPI. Hence, with pMRI it is possible to obtain images with reduced distortions as in segmented EPI, without the drawback of being sensitive to flow or motion or an increased acquisition time.

However, image reconstruction of single-shot EPI applications with SENSE is problematic because the distortions in EPI images and coil sensitivity maps are different. This means that the image intensity at a given location may not correspond to the correct value in the sensitivity map. Possible solutions have been reported to overcome this problem with SENSE.[18,19] However, GRAPPA has proven to be well suited for EPI, since the k-space based reconstruction of missing lines is not affected by image distortions. In almost every area tested so far, GRAPPA showed robust reconstructions without modifying either the EPI sequence or the reconstruction algorithm.[24] An example is shown in Figure 11.

In many applications, such as cardiac imaging, only a relatively small region within the object is relevant for a diagnosis. By choosing the FOV smaller than the object, so that the irrelevant parts of the image get aliased, the imaging speed at a constant resolution can be increased, even without parallel im-
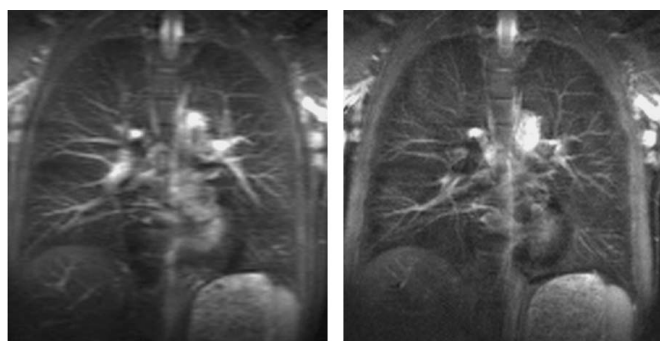
(a)   **(b)**

FIGURE 10. Single-shot HASTE imaging of the lung in combination with GRAPPA. A, Conventional HASTE image with a matrix size of 128 × 256 acquired in 220 ms (effective *TE* = 23 ms, T_{inter} = 2.88 ms, FOV = 500 mm × 500 mm), for this image 72 echoes were acquired. B, GRAPPA acquisition with an acceleration factor of 3. Compared with the reference image, the resolution is doubled, while the acquisition time is reduced from 220 ms to 161 ms (52 echoes were acquired).

aging. However, aliased full FOV images can cause discontinuities; therefore, erroneous coil sensitivity maps may be generated, leading to image artifacts after the reconstruction. To avoid this problem for SENSE-like methods, the FOV has to be larger than the object, preventing any aliasing of tissue from outside the FOV.[25] In contrast, GRAPPA is able to generate partially aliased image reconstructions, with the same appearance as in conventional imaging, without any modifications of the reconstruction algorithm (Fig. 12). An aliased full FOV image corresponds to a greater spacing in k-space than would be required by the Nyquist criterion. The spacing to the neighboring k-space lines, and hence the size of the FOV, is not
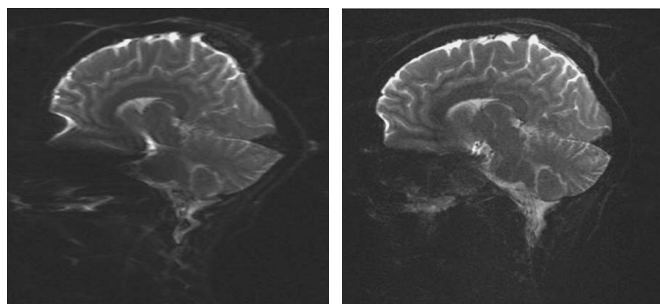
(a)   **(b)**

FIGURE 11. Reduced distortions in single-shot echo-planar imaging (EPI) by the use of pMRI, acquired with an eight-element head coil array. A, Conventional EPI with 128 × 256 matrix size and a minimal interecho spacing of T_{inter} = 1.4 ms. B, With GRAPPA using an acceleration factor of 3, the resolution is doubled to 256 × 256. Furthermore, this image shows reduced distortions, due to the reduced interecho spacing of T_{inter} = 0.37 ms.
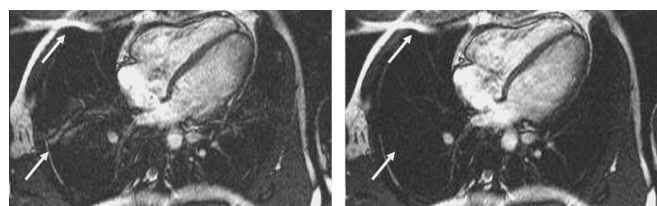

(a)   **(b)**

FIGURE 12. Image acquisitions with aliasing in the full FOV. A, An mSENSE reconstruction with an acceleration factor of 2. Aliasing in the full FOV causes artifacts in the reconstructed image as indicated by arrows. B, A GRAPPA reconstruction with an acceleration factor of 2 is shown. No artifacts can be seen in the reconstructed full FOV.

important for determining the signal for each individual line; therefore, the k-space lines are not corrupted by the use of a smaller FOV. Since the GRAPPA algorithm only involves fitting of neighboring k-space lines, this type of reconstruction is also unaffected by the smaller FOV, allowing an optimal FOV acceleration for a given application.

The differences between the two methods can be seen in the appearance of artifacts (Fig. 13). The SENSE reconstruction is performed in the image domain on a pixel-by-pixel basis. Nonideal conditioning in the reconstruction causes local noise enhancement and appears therefore localized in the unfolded image. In contrast, the GRAPPA algorithm generates the missing lines in k-space. An inaccurate calculation of the missing lines will produce aliasing artifacts in the reconstructed image, which can be seen over the entire reconstructed
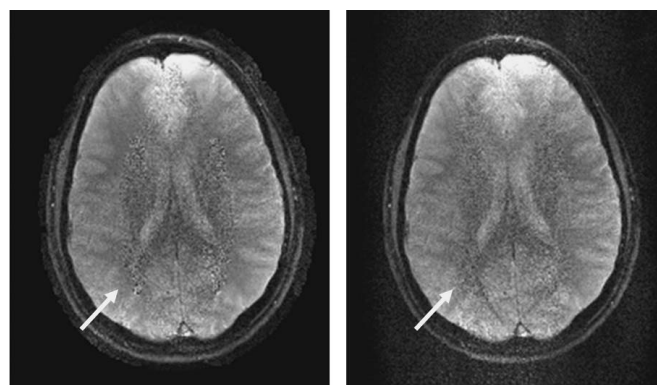
(a)   **(b)**

FIGURE 13. Comparison of artifacts in SENSE and GRAPPA reconstructions at very high accelerations (acceleration factor *R* is close to the number of coils N_c). In this example, a fourfold scan time reduction was achieved using only four coils. A, The SENSE image shows a local noise enhancement due to nonideal conditioning for the reconstruction. B, The noise enhancement in GRAPPA is distributed more evenly over the FOV. Additionally, aliasing artifacts can be seen due to inaccurate calculation of missing k-space lines.

FOV. It should be noted that aliasing artifacts can also be seen in SENSE due to errors in the coil sensitivity maps.

Coil Sensitivity Calibration

For accurate pMRI reconstructions, in vivo coil sensitivity calibrations are essential. Therefore, reference measurements have to be carried out to obtain this information.

This is commonly performed in vivo using a single 3D reference scan prior to the clinical examination. Typically, a low-resolution gradient echo sequence with short repetition time is used to acquire proton-density weighted images. Since the reference data are available in three dimensions and can be reformatted prior to the reconstruction, this permits accelerated scanning at any image plane orientation, interactive slice reorientation, and fast volume scanning. The prescan strategy is well suited for applications where no coil or patient motion is expected, for example, in head MRI, and allows the application of optimal acceleration factors. Problems with this prescan method might arise when the coil sensitivities across the object have changed between prescan and actual image acquisition, for example, when the patient moves between the different experiments.

As mentioned earlier, other approaches for coil sensitivity calibration include the auto- or self-calibrating methods. The idea is to record the coil sensitivity information directly during the actual scan by adding a small number of additionally acquired fully Fourier-encoded autocalibration lines. This direct sensitivity calibration for each image is beneficial in combination with flexible coil arrays or imaging of uncooperative patients. An accurate reconstruction is ensured, even if the coil or object position changes from scan to scan. Additionally, when multiple receiver coil systems are combined, for example, for whole-body screening, the autocalibration method relaxes the requirements for the application of parallel imaging.[26]

A drawback of this strategy is the decrease in data acquisition efficiency, which can lead to lower frame rates in dynamic imaging because the total acquisition time for an image is increased by a small amount. However, for breath-hold studies, such as cine imaging, the autocalibration data only have to be recorded in one frame and, therefore, most of the acquisition efficiency can be retained.[27] Optimized autocalibrated methods for dynamic imaging, such as TSENSE[28] or TGRAPPA,[29] extract the sensitivity calibration information directly from the recorded data itself by incorporating an interleaved k-space acquisition scheme (ie, UNFOLD).[30] No further information is needed for image reconstruction, therefore avoiding the reduction of the overall acceleration. Figure 14 illustrates the influence of inaccurate sensitivity calibration due to the presence of respiratory motion in a real-time non-breath-held cardiac imaging study and highlights the rational for autocalibration. Respiratory motion can significantly change the position of a flexible coil array, leading to residual
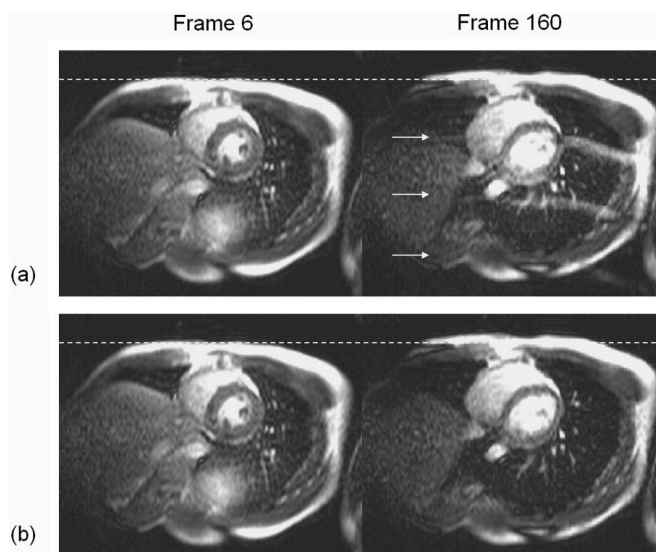

FIGURE 14. Illustration of the influence of inaccurate sensitivity information on a successful pMRI reconstruction. Two time frames (frame 6, frame 160) are shown from an accelerated (R = 4) real-time TrueFISP non–breath-held dynamic cardiac imaging experiment with a temporal resolution of 30 frames per second. The image reconstructions were done using the GRAPPA algorithm with reference signals taken (A) only once at the beginning of the series and (B) dynamically updated during the series. It can be seen that respiratory motion can significantly change the position of the flexible coil array from the original position (indicated by the dashed lines), resulting in residual artifacts in time frames where the reference data for coil calibration do not match the actual coil position. Siemens Sonata 1.5 Tesla whole body scanner, 8-channel coil from NOVA Medical, *TE* = 1.11 ms, *TR* = 2.22 ms, FOV = 36.0 cm × 29.2 cm, 8-mm slice thickness, matrix = 128 × 60, α = 50°. These data were kindly provided by Peter Kellman from NIH/NHLBI.

artifacts in time frames where the reference data for coil calibration do not match the actual coil position. These artifacts disappear if the reconstruction parameters are updated dynamically for each time frame, as shown in Figure 14. In this case, it is clear that the autocalibration method provides results that are superior these obtained with a prescan.

It is important to note that the method for coil sensitivity calibration is independent from the reconstruction algorithm. In its first implementations, SENSE used the prescan strategy for coil sensitivity assessment and GRAPPA employed the autocalibration method. However, in principle, both reconstruction techniques can be performed using either the prescan or the autocalibration method to obtain the coil sensitivity information. The mSENSE implementation, for example, uses the autocalibration strategy for coil sensitivity assessment.[7]

DISCUSSION

In this review article, we have tried to give some answers to the question of which pMRI method is optimal for a given

specific application. Therefore, we have given a brief technical overview of the existing parallel imaging techniques and worked out differences, similarities, advantages, and disadvantages of the various methods. Because, at present, the only commercially available pMRI techniques for clinical applications are SENSE and GRAPPA, the main focus of this article was put on these two methods.

The first successful in vivo pMRI implementation, SMASH, was introduced in 1997. Since then, new approaches have been proposed to perform in vivo parallel imaging more robust and with less effort. All modern parallel imaging methods can be categorized into three groups, namely, image domain-based techniques (SENSE, PILS), regenerative k-space methods (SMASH, AUTO-SMASH, GRAPPA), and hybrid techniques (SPACE RIP, Generalized SENSE).

In summary, only SENSE and GRAPPA are commercially available for clinical applications. Both techniques are well suited to enhance virtually every MRI application. In our experience, there is no absolute advantage of one or the other method. Both techniques allow an accelerated image acquisition in arbitrary image plane orientation as well as with arbitrary coil configurations with essentially the same SNR performance. In our experience, GRAPPA has a slight advantage in inhomogeneous regions with low spin density, such as the lung and in single-shot EPI in regions of severe distortions.

Furthermore, aliasing in the reconstructed full FOV is not a problem with GRAPPA, therefore allowing an optimal FOV acceleration for a given application. However, whenever an accurate coil sensitivity map can be obtained, SENSE provides the best possible reconstruction with optimized SNR and shows slightly better image quality than GRAPPA in very highly accelerated applications, with acceleration factors in the order of the number of coils.

In general, all parallel imaging methods are expected to benefit from more coil array elements. Recently, MR systems with up to 32 channels have become available. However, for most clinical applications, a limitation of the acceleration factor is expected. The main reason for this is the SNR degradation by a factor of the square root of the acceleration factor due to the reduced scan time. Additionally, for higher accelerations, the aliased points move closer together and because of the slowly varying coil sensitivities, the ability to separate superimposed pixels decreases. This leads to an additional spatially dependent noise amplification, which is indicated by an increased g-factor.[2] In two-dimensional parallel imaging, data reduction is performed along one dimension, the phase-encoding direction. It is expected that for clinical applications the acceleration factor in 2D imaging will not exceed a factor of 4 or 5.[31] In 3D MRI, undersampling can be carried out along two dimensions: the phase-encoding and the 3D direction. A higher scan time reduction can be achieved in this way because 1) the intrinsic SNR is relatively high and 2) the encoding efficiency is improved, since coil sensitivity variations can be exploited along two dimensions. For 3D imaging, we expect a maximum achievable acceleration factor of about 16, assuming that appropriate coil arrays are available.

Look Into the Future

Since its introduction in the late 1990s, parallel imaging techniques have been improved over the last years, and achieved higher acceleration factors, robust coil sensitivity calibration methods, and improved reconstruction algorithms. More advanced generations of pMRI scanners will be equipped with more receiver coils and new concepts of image acquisition and reconstruction techniques and will broaden the influence of parallel imaging on the clinical routine. In the following section, new advances in pMRI are described which might be affecting daily clinical diagnosis in the near future.

Dynamic Parallel Imaging With k-t-SENSE, TSENSE, and TGRAPPA

An area that is particularly interesting for the application of pMRI is dynamic imaging. The primary goal in these applications is to simply acquire images as fast as possible with enough SNR to observe the object of interest.

The TSENSE method[28] is based on a time-interleaved k-space acquisition scheme as in the UNFOLD technique.[30] Here the sequence acquisition for the individual time frames alternates between even and odd k-space lines achieving an acceleration factor of 2 for each frame. Coil sensitivities are derived from full FOV images obtained by combining two adjacent time frames. Since one time frame contains all odd lines and the next time frame contains all even lines, stacking together both fames leads to a complete k-space data set. Therefore, the TSENSE method does not require a separate image acquisition for coil sensitivity estimation and is able to tolerate coil or body motion. Additionally, temporal low-pass filtering of the reconstructed images provides a high degree of artifact suppression of residual aliasing components.

Similar to TSENSE, the k-space-based TGRAPPA method has been introduced.[29] By using the time interleaved acquisition scheme as described above, a full k-space data set can be assembled from adjacent time frames to obtain the coil sensitivity calibration information. The calibration information can be updated dynamically and enables robust reconstructions with high image quality even in cases where coils are moving during data acquisition. Although excellent artifact suppression has been demonstrated, an optional temporal filter as in TSENSE can be applied to TGRAPPA to further suppress residual artifacts.

Both TSENSE and TGRAPPA are particularly interesting for real-time applications, such as free-breathing cardiac imaging or accelerated interventional MRI.

Recently, the k-t-SENSE[32] method has been presented, which exploits signal correlations in both k-space and time to recover the missing data. Based on a training data set, a regu-

larized spatiotemporal filter allows higher imaging accelerations and therefore higher temporal resolution. This method is especially applicable to areas with objects that exhibit a quasi-periodic motion, such as the heart and the brain under periodic stimulation.

Non-Cartesian Parallel MRI

Another field of research at present is the use of parallel imaging in combination with non-Cartesian k-space trajectories, such as spiral or radial sampling. Compared with the conventional Cartesian sampling pattern, non-Cartesian sampling schemes offer distinct advantages for MRI in many cases.

However, the combination with parallel imaging is non-trivial because, in general, large systems of linear equations have to be solved. Yet an efficient iterative reconstruction procedure combining SENSE with arbitrary k-space trajectories has been presented, which allow reconstruction on the order of a few seconds for most applications.[33–36]

For the special case of radial sampled data, it has been shown that missing projections can directly be reconstructed with a conventional GRAPPA algorithm when different reconstruction weights are used along the read-out direction.[37] The main advantage is the relatively short reconstruction time for dynamic imaging, since the reconstruction parameters have to be determined for only one time frame and can be applied to all of the following data. In an equivalent way, this concept also works for segmented spiral k-space trajectories.[38]

Non-Cartesian parallel imaging based on the PILS technique is also a topic at research sites. The main benefit of using PILS in combination with radial or spiral k-space scanning is the relatively low computational complexity for the image reconstruction. Good results have been presented for both spiral and radial applications up to accelerations of 2 to 3.[39,40]

CONCLUSION

In this review article, a brief technical overview of all modern pMRI methods was given and differences and similarities as well as advantages and disadvantages have been worked out to help in choosing the optimal parallel imaging method for a specific clinical application. In general, most modern pMRI methods will result in similar image quality for most applications, while some specific application may benefit from specialized pMRI approaches. However, it is clear that pMRI methods have the potential to impact nearly every area of clinical MRI.

ACKNOWLEDGMENTS

REFERENCES

1. Sodickson DK, Manning WJ. Simultaneous acquisition of spatial harmonics (SMASH): fast imaging with radiofrequency coil arrays. *Magn Reson Med*. 1997;38:591–603.
2. Pruessmann KP, Weiger M, Scheidegger MB, et al. SENSE: sensitivity encoding for fast MRI. *Magn Reson Med*. 1999;42:952–962.
3. Griswold MA, Jakob PM, Heidemann RM, et al. Generalized autocalibrating partially parallel acquisitions (GRAPPA). *Magn Reson Med*. 2002;47:1202–1210.
4. Jakob PM, Griswold MA, Edelman RR, et al. AUTO-SMASH: a self-calibrating technique for SMASH imaging: SiMultaneous Acquisition of Spatial Harmonics. *MAGMA*. 1998;7:42–54.
5. Heidemann RM, Griswold MA, Haase A, et al. VD-AUTO-SMASH imaging. *Magn Reson Med*. 2001;45:1066–1074.
6. Bydder M, Larkman DJ, Hajnal JV. Generalized SMASH imaging. *Magn Reson Med*. 2002;47:160–170.
7. Wang J, Kluge T, Nittka M, et al. Parallel acquisition techniques with modified SENSE reconstruction mSENSE. *Proceedings of the First Würzburg Workshop on Parallel Imaging Basics and Clinical Applications*, Würzburg, Germany, 2001:89.
8. Griswold MA, Jakob PM, Nittka M, et al. Partially parallel imaging with localized sensitivities (PILS). *Magn Reson Med*. 2000;44:602–609.
9. Kyriakos WE, Panych LP, Kacher DF, et al. Sensitivity profiles from an array of coils for encoding and reconstruction in parallel (SPACE RIP). *Magn Reson Med*. 2000;44:301–308.
10. Sodickson DK. Tailored SMASH image reconstructions for robust in vivo parallel MR imaging. *Magn Reson Med*. 2000;44:243–251.
11. de Zwart JA, van Gelderen P, Kellman P, et al. Application of sensitivity-encoded echo-planar imaging for blood oxygen level-dependent functional brain imaging. *Magn Reson Med*. 2002;48:1011–1020.
12. Bydder M, Larkman DJ, Hajnal JV. Combination of signals from array coils using image-based estimation of coil sensitivity profiles. *Magn Reson Med*. 2002;47:539–548.
13. Walsh DO, Gmitro AF, Marcellin MW. Adaptive reconstruction of phased array MR imagery. *Magn Reson Med*. 2000;43:682–690.
14. Pruessmann KP, Weiger M, Boesiger P. Sensitivity encoded cardiac MRI. *J Cardiovasc Magn Reson*. 2001;3:1–9.
15. Weiger M, Pruessmann KP, Boesiger P. Cardiac real-time imaging using SENSE. SENSitivity encoding scheme. *Magn Reson Med*. 2000;43:177–184.
16. Weiger M, Pruessmann KP, Kassner A, et al. Contrast-enhanced 3D MRA using SENSE. *J Magn Reson Imaging*. 2000;12:671–677.
17. Griswold MA, Jakob PM, Chen Q, et al. Resolution enhancement in single-shot imaging using simultaneous acquisition of spatial harmonics (SMASH). *Magn Reson Med*. 1999;41:1236–1245.
18. Bammer R, Auer M, Keeling SL, et al. Diffusion tensor imaging using single-shot SENSE-EPI. *Magn Reson Med*. 2002;48:128–136.
19. Bammer R, Keeling SL, Augustin M, et al. Improved diffusion-weighted single shot echo-planar imaging (EPI) in stroke using sensitivity encoding (SENSE). *Magn Reson Med*. 2001;46:548–554.
20. Larkman DJ, deSouza NM, Bydder M, et al. An investigation into the use of sensitivity-encoded techniques to increase temporal resolution in dynamic contrast-enhanced breast imaging. *J Magn Reson Imaging*. 2001;14:329–335.
21. Heidemann RM, Griswold MA, Kiefer B, et al. Resolution enhancement in lung 1H imaging using parallel imaging methods. *Magn Reson Med*. 2003;49:391–394.
22. Fink C, Bock M, Puderbach M, et al. Contrast enhanced 3D MR perfusion imaging of the lungs using parallel imaging techniques. *Proceedings of the 11th Annual Meeting of the ISMRM*, Toronto, 2003:1366.
23. Wintersperger BJ, Nikolaou K, Schoenberg SO, et al. Single breath-hold real-time evaluation of cardiac function: improvement of temporal resolution using generalized autocalibrating partially parallel acquisition (GRAPPA) algorithms. *Proceedings of the 11th Annual Meeting of the ISMRM*, Toronto, 2003:1587.
24. Heidemann RM, Griswold MA, Porter D, et al. Minimizing distortions and blurring in diffusion weighted single shot EPI using high performance

gradients in combination with parallel imaging. *Proceedings of the 9th Annual Meeting of the ISMRM*, Glasgow, 2001:169.

25. Goldfarb JW, Shinnar M. Field-of-view restrictions for artifact-free SENSE imaging. *Proceedings of the 10th Annual Meeting of the ISMRM*, Honolulu, 2002:2412.

26. Quick HH, Vogt F, Herborn CU, et al. High-resolution whole-body MR angiography featuring parallel imaging. *Proceedings of the 11th Annual Meeting of the ISMRM*, Toronto, 2003:254.

27. Zhang Q, Park J, Li D, et al. Improving true-FISP parallel cine imaging using a new data-acquisition scheme for coil sensitivity calibration. *Proceedings of the 11th Annual Meeting of the ISMRM*, Toronto, 2003:2329.

28. Kellman P, Epstein FH, McVeigh ER. Adaptive sensitivity encoding incorporating temporal filtering (TSENSE). *Magn Reson Med*. 2001;45:846–852.

29. Breuer F, Kellman P, Griswold MA, et al. Dynamic autocalibrated imaging using TGRAPPA. *Proceedings of the 11th Annual Meeting of the ISMRM*, Toronto, 2003:2330.

30. Madore B, Glover GH, Pelc NJ. Unaliasing by Fourier-encoding the overlaps using the temporal dimension (UNFOLD), applied to cardiac imaging and fMRI. *Magn Reson Med*. 1999;42:813–828.

31. Ohliger MA, Grant AK, Sodickson DK. Ultimate intrinsic signal-to-noise ratio for parallel MRI: electromagnetic field considerations. *Magn Reson Med*. 2003;50:1018–1030.

32. Tsao J, Boesiger P, Pruessmann KP. k-t BLAST and k-t SENSE: dynamic MRI with high frame rate exploiting spatiotemporal correlations. *Magn Reson Med*. 2003;50:1031–1042.

33. Pruessmann KP, Weiger M, Boernert P, et al. A gridding approach for sensitivity encoding with arbitrary trajectories. *Proceedings of the 8th Annual Meeting of the ISMRM*, Denver, 2000:276.

34. Pruessmann KP, Weiger M, Börnert P, et al. Advances in sensitivity encoding with arbitrary k-space trajectories. *Magn Reson Med*. 2001;46:638–651.

35. Kannengießer SAR, Brenner AR, Noll TG. Accelerated image reconstruction for sensitivity encoded imaging with arbitrary k-space trajectories. *Proceedings of the 8th Annual Meeting of the ISMRM*, Denver, 2000:155.

36. Weiger M, Pruessmann KP, Österbauer R, et al. Sensitivity-encoded single-shot spiral imaging for reduced susceptibility in BOLD fMRI. *Magn Reson Med*. 2002;48:860–866.

37. Griswold MA, Heidemann RM, Jakob PM. Direct parallel imaging reconstruction of radially sampled data using GRAPPA with relative shifts. *Proceedings of the 11th Annual Meeting of the ISMRM*, Toronto, 2003:2349.

38. Heberlein KA, Kadah Y, Hu X. Segmented spiral parallel imaging using GRAPPA. *Proceedings of the 12th Annual Meeting of the ISMRM*, Kyoto, Japan, 2004:328.

39. Eggers H, Boernert P, Boesiger P. Real-time partial parallel spiral imaging with localized sensitivities. *Proceedings of the 9th Annual Meeting of the ISMRM*, Glasgow, 2001:1772.

40. Härer W, Mertelmeier T, Oppelt A. Accelerated projection reconstruction by parallel acquisition. *Proceedings of the First Würzburg Workshop on Parallel Imaging Basics and Clinical Applications*, Würzburg, Germany, 2001:91.